Accepted Manuscript

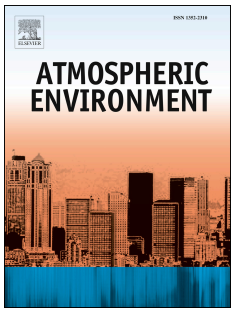

Global assessment of shipping emissions in 2015 on a high spatial and temporal resolution

Lasse Johansson, Jukka-Pekka Jalkanen, Jaakko Kukkonen

PII: S1352-2310(17)30556-3

DOI: 10.1016/j.atmosenv.2017.08.042

Reference: AEA 15512

To appear in: *Atmospheric Environment*

Received Date: 18 April 2017

Revised Date: 14 August 2017

Accepted Date: 17 August 2017

Please cite this article as: Johansson, L., Jalkanen, J.-P., Kukkonen, J., Global assessment of shipping emissions in 2015 on a high spatial and temporal resolution, *Atmospheric Environment* (2017), doi: 10.1016/j.atmosenv.2017.08.042.

Global assessment of shipping emissions in 2015 on a high spatial and temporal resolution

Lasse Johansson[1], Jukka-Pekka Jalkanen[1] and Jaakko Kukkonen[1]

[1]Finnish Meteorological Institute (FMI), Erik Palmenin aukio 1, 00101 Helsinki, Finland
Corresponding author: Lasse Johansson, lasse.johansson@fmi.fi

Abstract

We present a comprehensive global shipping emission inventory and the global activities of ships for the year 2015. The emissions were evaluated using the Ship Traffic Emission Assessment Model (STEAM3), which uses Automatic Identification System data to describe the traffic activities of ships. We have improved the model regarding (i) the evaluation of the missing technical specifications of ships, and (ii) the treatment of shipping activities in case of sparse satellite AIS-data. We have developed a model for the collection and processing of available information on the technical specifications, using data assimilation techniques. We have also developed a path regeneration model that constructs, whenever necessary, the detailed geometry of the ship routes. The presented results for fuel consumption were qualitatively in agreement both with those in the 3rd Greenhouse Gas Study of the International Maritime Organisation and those reported by the International Energy Agency. We have also presented high-resolution global spatial distributions of the shipping emissions of NO_x, CO_2, SO_2 and $PM_{2.5}$. The emissions were also analysed in terms of selected sea areas, ship categories, the sizes of ships and flag states. The emission datasets provided by this study are available upon request; the datasets produced by the model can be utilized as input data for air quality modelling on a global scale, including the full temporal and spatial variation of shipping emissions for the first time. Dispersion modelling using this inventory as input can be used to assess the impacts of various emission abatement scenarios. The emission computation methods presented in this paper could also be used, e.g., to provide annual updates of the global ship emissions.

Keywords: Global shipping emissions, AIS, shortest path networks, CO2, STEAM

1. Introduction

Reliable and detailed emission inventories are crucial for the accuracy of air quality modelling; such inventories should include all sectors of anthropogenic and non-anthropogenic pollution. Information on emissions should also include a sufficiently detailed treatment of their geographical and temporal variations. The introduction of an automatic vessel position reporting system, called the Automatic Identification System (AIS), has significantly reduced the uncertainties concerning ship activities. Currently, all vessels larger than 300 tons globally report their position with a few second intervals.

The use of Automatic Identification System (AIS) data for the assessment of shipping emissions has substantially increased during the last few years. Both the geographical coverage achieved via AIS satellite receivers and the amount of usable AIS-based shipping activity data have substantially increased while the financial costs for acquiring the relevant AIS data have significantly decreased. The availability of the new data has made it possible to use refined

methods that can significantly improve the quality of bottom-up ship emission inventories. The main advantage of such bottom-up emission inventories, compared to the top-down ones, is that these can describe the emitters in a more realistic manner, while maintaining the connection between single emitters and large scale inventories. In addition, it is possible to construct sophisticated emission scenarios and analyze in detail the spatial-temporal variation of emissions.

The AIS system is useful for the evaluation of ship emissions, as it provides continuously automatic information on the vessel positions and instantaneous speeds of ships. If the required vessel characteristics are also known, the exhaust emissions can be modelled on very high temporal and spatial resolutions. The ship emission inventories based on the use of the AIS signals have several significant advantages over the previously developed approaches (e.g., Smith et al., 2015, Jalkanen et al., 2016). Such inventories are based on time-dependent, high-resolution dynamic traffic patterns, which can also allow, e.g., for the effects of changing weather conditions.

The function of AIS-data as a means to estimate shipping emissions is not new; AIS has been used previously for the assessment of emissions and air pollution originated from shipping. However, the scope of these studies has commonly been limited either to city-scale, for instance, regarding the influence of harbours and nearby ship traffic, or to selected sea regions (e.g., Jalkanen et al., 2012; Johansson et al., 2013, Liu et al., 2016, Marelle et al., 2016, Goldsworthy et al, 2015, Song, 2014, Ng et al., 2013, Matthias et al., 2016, Aulinger et al., 2016). There is one exception: in the Third Greenhouse Gas (GHG) Study of the International Maritime Organisation (IMO; Smith et al, 2015), AIS-data was used to assess global shipping emissions. Before the present study, the Third GHG Study therefore represented the most detailed and comprehensive global inventory of shipping emissions. The aim of that study was to provide IMO with both a multi-year inventory and future scenarios for green-house gases and other emissions from ships. Analysis in that study was carried out for each ship during each hour of each of the years 2007–2012, before aggregation to evaluate the total values. Since the focus of that study was on the evaluation of the total shipping emissions, the authors did consider neither the realistic pathing of individual ships nor the resulting spatial- and temporal variability of global shipping emissions. However, an accurate representation of the spatial and temporal variability the global shipping emissions is crucial for air quality modelling purposes.

Corbett et al. (2007) analysed the global premature mortality caused by ship emissions. They evaluated that shipping-related PM emissions were annually responsible for a considerable amount, approximately 60,000, cardiopulmonary and lung cancer deaths. The impacts were focused in coastal regions on major trade routes; most premature deaths occurred near coastlines in Europe, East Asia and South Asia. Liu et al. (2016) evaluated the health and climate impacts of vessels in East Asia, using a detailed bottom-up AIS-based shipping emission model. They reported that shipping emissions in East Asia had rapidly increased since the beginning of this century. According to that study, East Asia accounted for 16 % of global shipping CO_2 emissions in 2013, compared to only 4–7 % in 2002–2005. Further, the emissions from shipping in East Asia resulted in substantial adverse health impacts, with 14,500–37,500 premature deaths per year according to Liu et al. Since the data regarding the technical characteristics of vessels can be difficult to obtain, especially for smaller vessels, Liu et al. adopted Gradient Boosting Regression Trees (GBRT) to refine their technical vessel database. Despite the adopted GBRT technique, the amount of identified and technically specified vessels was limited to 18,300 ships; the clear majority of AIS-messages (3.7 billion of 5.7 billion) originated from ships that could not be identified and were omitted from the modelling.

The present authors have previously introduced the Ship Traffic Emission Assessment Model (STEAM), which uses AIS data to describe ship traffic activity. The previous model versions have been described in detail by Jalkanen et al. (2009, 2012, 2014 and 2016) and

Johansson et al. (2013). The model has previously been applied to evaluate the shipping emissions in the Baltic Sea (Jalkanen et al., 2009), in the Danish Straits (Jalkanen et al., 2012), in the Baltic and North Seas (Johansson et al., 2013; Jonson et al., 2016), and in the whole of Europe (Jalkanen et al., 2016).

In this study, we present for the first time a global, entirely bottom-up, physically realistic AIS-based assessment of shipping emissions on very high spatial and temporal resolutions. Our modelling approach is based on the vessel water resistance method (Hollenbach, 1998). We model the shipping activities of each vessel that send AIS-data and consider the activities of ships between the consecutive AIS-messages on a minute by minute basis. We have constructed a route generation algorithm to handle the challenges related to the sparsity and heterogeneous distribution of AIS-data. Further, we use data-assimilation techniques to assign physically realistic properties for ships, for which the technical information is incomplete or missing. We included non-IMO registered traffic in our modelling; for each ship we included also the temporally resolved effects related to emission control areas and emission abatement equipment installed on-board. The final results can readily be used as input values for atmospheric dispersion models.

The first aim of this study is to describe the latest improvements of the applied mathematical emission model (called STEAM3), especially focusing on two key improvements that were required to perform the global assessments. The second aim is to inter-compare the numerical results on the fuel consumption to the values reported in the corresponding previous inventories. The third aim is to present new selected numerical results on the activities and atmospheric emissions of global shipping. We have not presented an evaluation of the STEAM3 model against measured emission or concentration data in this paper; that has been addressed extensively in several previous studies (e.g., Jalkanen et al., 2009, 2012, 2014 and 2016; Johansson et al., 2013; Marelle et al., 2016).

2. Methods

The STEAM model combines the AIS-based information and the detailed technical knowledge of the world fleet with principles of naval architecture. This input information is used to predict the resistance of vessels in water and the instantaneous engine power of the main and auxiliary engines on a minute-by-minute basis, for each vessel that has sent AIS messages. The model then predicts as output both the instantaneous fuel consumption and the emissions of selected pollutants (Jalkanen et al., 2012; Johansson et al., 2013).

In the following, we introduce a refined version of the Ship Traffic Emission Assessment Model (STEAM3) and describe the improvements of the model that were required for the global assessments. These include the methods that compensate for (i) the missing information on the technical specifications of a fraction of the ships and (ii) the scarcity of satellite data in some regions. In addition, we address (iii) the model refinements that allow for the modelling of international emission control areas, the use of scrubbers and dual fuel systems. In this study we have used the commercial AIS messages, both terrestrial and satellite-based, provided by Orbcomm[1] for the year of 2015. Detailed vessel characteristics have been gathered for more than 90,000 individual ships, reported by IHS Fairplay and other ship classification societies.

The main components of the modelling approach, which are applied separately to each ship, have been schematically presented in Figure 1. The modelling can be broadly classified to three stages. In the first stage, the relevant data is gathered from various sources, assimilated and pre-processed. In this initial process we have first combined all ship activity data from multiple

[1]Orbcomm, 395 W Passaic Street, Suite 325, Rochelle Park, NJ 07662 USA, 2017.

sources, and then sorted the data chronologically. We have next identified the possible significant spatial and temporal gaps in the vessel specific activity dataset, and applied route generation algorithms to better process the information contained in the activity data (Section 2.2). For the most vessels there were also missing technical details, which can be either missing data fields or completely missing entries in the ship database. Such missing entries have been replaced based on (i) the technical information derived from selected sources in the www, (ii) the information in the static AIS-data and (iii) an algorithm that replicates the missing information based on a similar vessel listed in the database (Section 2.1).

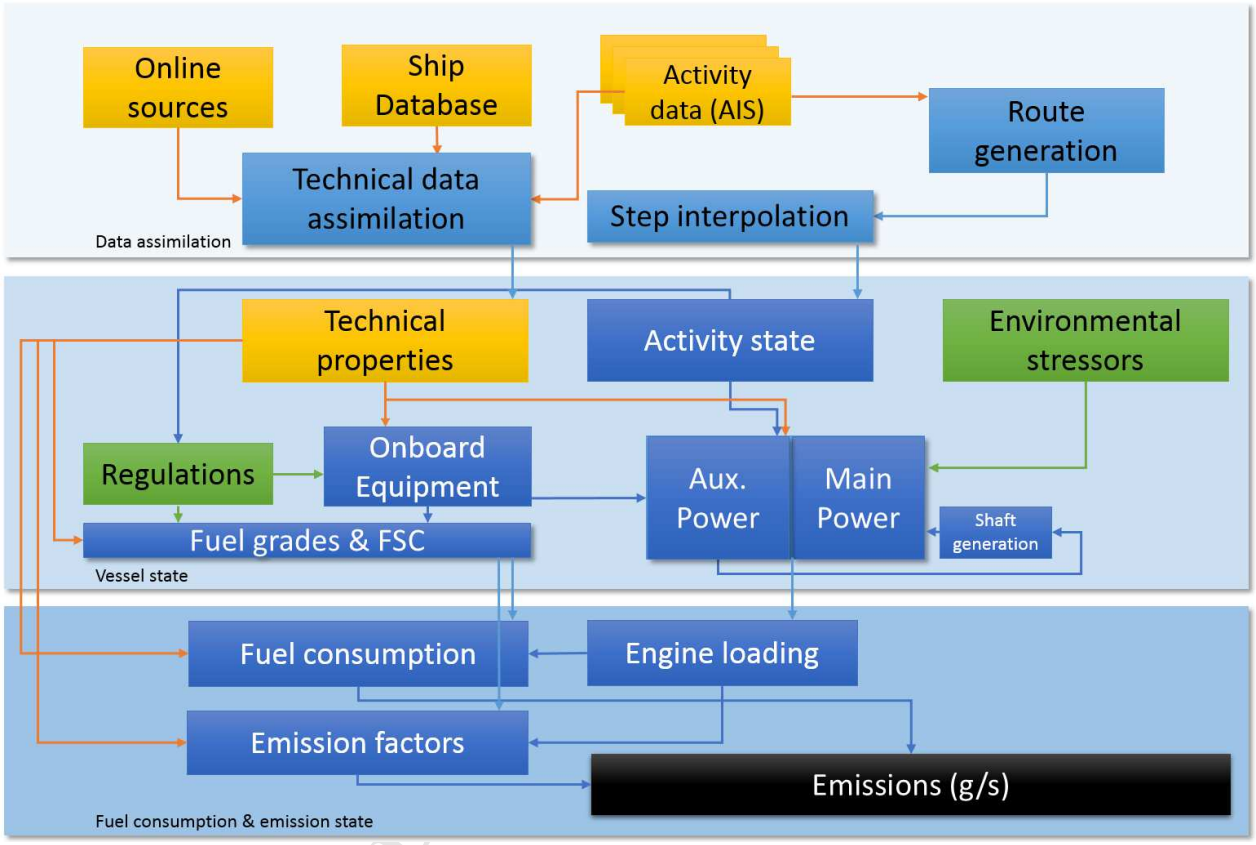

Figure 1: Schematic diagram of the modelling approach and the three stages of modelling (data collection, assimilation and pre-processing; vessel properties and state evaluation; fuel consumption and emissions evaluation). The yellow colour refers to the input data, green to external factors, light blue to pre-processing and dark blue indicates individual model components.

After the technical properties have been assimilated and the shipping routes have been generated, the second stage is to assess the state of the vessel on a minute-by-minute basis. In this stage, the main goal is to estimate the required power outputs for engines, as well as the used fuel grades and their fuel sulphur content. However, there are numerous interdependent factors that affect the outcome of this assessment. The activity state (which we define to include the location, time, speed, acceleration, operational mode, and the berthing time counter) and the technical details of the vessel are used to assess the initial required power output; this is done separately for the main and auxiliary engines. Environmental factors, such as waves, sea currents and ice cover, can increase the required main power, but the influence of such factors was not taken into account in this study. The combination of these factors, when taken into account, could increase the global annual fuel consumption estimates by as much as 5-15 percent.

If the ship can generate auxiliary power with shaft generators or uses diesel-electric principle for power transmission, then the auxiliary power requirement will be allocated to the main engine. The model is then used to evaluate the fuel grades consumed by each engine, and the fuel sulphur contents (FSC). This evaluation takes into account the technical limitations of the engines and the local emission regulations, as well as the availability of emission abatement equipment. For instance, in emission control areas the use of an operational open-loop scrubber facilitates the use of a cheaper fuel that has a higher FSC. The additional auxiliary power required for the use of the scrubber is also taken into account.

In the third stage, the engine loading, the fuel consumption and the emissions are computed. The model is also used to evaluate which engines are operational, and what are their balanced loads. The instantaneous fuel consumption and exhaust emissions are then computed based on the technical engine details, the load factors, the fuel grade and the abatement equipment (Jalkanen et al., 2012).

2.1 Evaluation of the technical specifications of vessels

Only a minority of the number of ships that send AIS-messages have a unique IMO identification number that can be used to associate the proper technical specifications to these vessels. In addition, even the IMO-registered vessels have in some cases incomplete specifications, e.g., there may be no information on auxiliary engines. In previously published studies, averages of vessel types have therefore been used to complete the missing entries. However, using the averages of vessel types will in a notable fraction of cases result in substantially inaccurate values (Appendix A). In Liu et al., 2016 this issue was addressed by using Gradient Boosting Regression Trees (GBRT) to refine their existing technical database. In this study, we propose another method that does not rely on the averages of vessel types. We complete the missing entries regarding ship technical specification by searching a so-called most similar vessel (MSV) in the ship properties database. Additionally, we extract vessel specifications from internet sources and static AIS-data so that the proposed search algorithm can also be utilized for the sizable global non-IMO registered fleet.

The MSV search process has been defined to proceed as follows. First, a list of possible MSV's is compiled, containing all ships of the same type as the ship, for which the technical data is incomplete. For each of these candidate ships, a measure of difference is computed, based on the relative differences of the length of ship (LOA) and the design speed between the candidate ship and the ship in question. The candidate ship with the smallest difference measure is selected as the MSV. The missing technical entry is then replaced by the information reported for the MSV.

The difference measure s is defined as

$$s = \sqrt{a\left(\frac{v - v_c}{v_c}\right)^2 + \left(\frac{l - l_c}{l_c}\right)^2} \qquad (1)$$

where v is the design speed of the ship, v_c is the design speed of the candidate ship, l is the ship's length (LOA), l_c is the candidate ship's length and $a = 0.35$. The empiric weighting factor a has been optimized using Monte Carlo –simulations, based on a large number of known ship entries in the ship properties database. Both the estimation of the factor a and an evaluation of the overall performance of the MSV search algorithm have been presented in Appendix A.

In order to use the MSV search for an unknown, presumably small vessel, at least the length, design speed and type of vessel must be known. Unfortunately, these pieces of information are not usually available. To address this issue we have produced an additional Maritime Mobile Service Identity (MMSI) -linked technical database using the information from several billion static AIS-messages included in the Orbcomm data for 2015 and a web crawler that uses the Bing search engine and systematically browses the World Wide Web. In case the static AIS-data contains insufficient amount of technical information the vessel's MMSI number is used as the search keyword in Bing. The web crawler follows links to the listed web pages and parses numerical values after identified key words, such as 'length', 'breadth', 'size' and 'type'. The details for the web crawler have been presented in Supplements A, including a performance evaluation using 100 randomly selected vessels.

2.2 Assessment of the routes of vessels in case of scarce data

For regions that are covered only by the satellite-based AIS data and there are no terrestrial receivers nearby, the input data for the modelling can be scarce: the geographical distance between two consecutive AIS-messages can be thousands of kilometres for a selected vessel. For each pair of consecutive messages we apply physical feasibility checks and corrections to determine the activities between the two activity points (Johansson et al., 2013). However, an attempt to interpolate the activities in the shipping routes using, e.g., great-circle paths may result in an unrealistic situation, in which the route would cross over land areas. In fact, any two consecutive route points that are spatially close to each other could actually be associated to a much longer travel route across the seas. To address this issue, a route generation algorithm has been developed and implemented to the STEAM3 model which can be used to evaluate the non-trivial route segments.

For the route generation, we have used a Dijkstra algorithm to determine the shortest path network (Cherkassky et al, 1996), which was also used for this purpose by Paxian et al (2009). A more detailed description of the route generation algorithm has been presented in Appendix B. The basic principle of this method has been illustrated in Fig 2. First, we use the STEAM3 model to determine the geographical distribution of the fuel consumption of the IMO-registered vessels, without using the route generation algorithm. The resulting gridded fuel consumption data, in which the shipping lanes are clearly visible, is used as a basis to describe the shipping routes as a series of coordinate points. Together the described shipping routes form a vast network of interconnected routes; the total length of the network is 1.04 million kilometres and is formed by 4,900 nodes and 12,300 arcs that connect the nodes to each other. Thus the network facilitates approximately 12 million unique node-to-node shortest path routes.

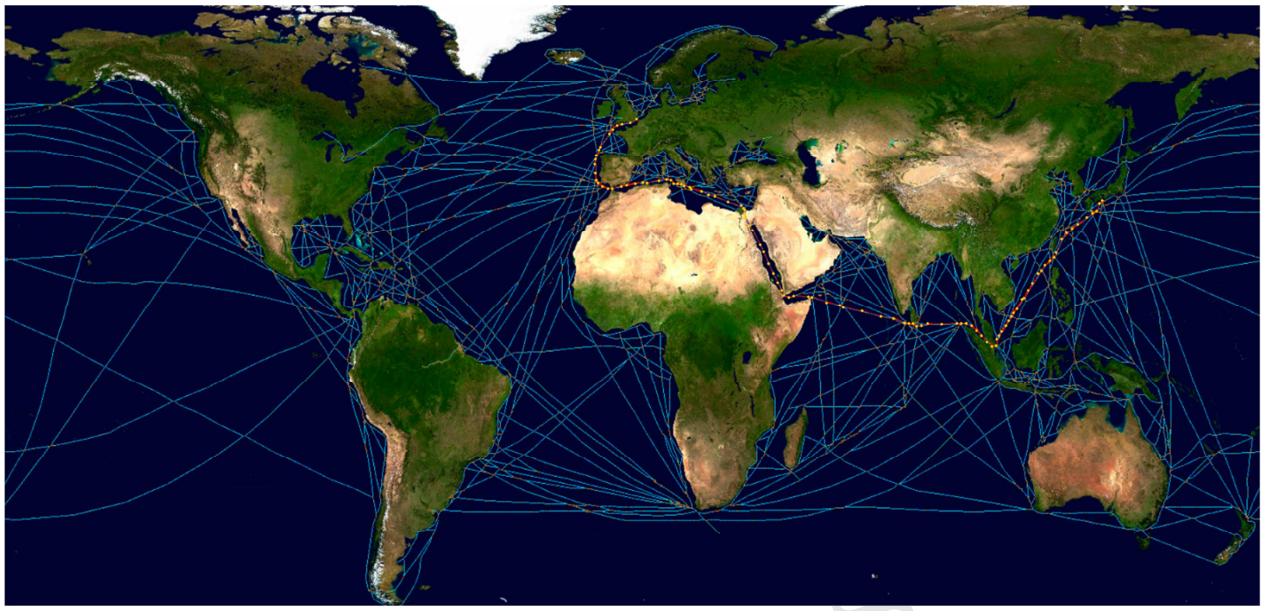

Figure 2: The network of nodes and arcs (light blue lines) that facilitate the Dijkstra algorithm for the assessment of shortest possible shipping routes. An example route given by the algorithm is shown, a sequence of nodes (yellow dots) and arcs (red lines) between a location near the English Channel and a location near Japan.

In brief, the algorithm is used as follows: first, based on the two consecutive AIS-messages it is evaluated whether or not the segment needs sophisticated path generation (e.g, there exists a significant amount of land mass between the points). Second, in case the route generation is needed, the closest nodes to the start point and the end point of the activity segment are identified. Third, the shortest path between the start node and the end node is evaluated with the Djikstra algorithm. Finally, additional proxy AIS-messages are generated in between the first and the last AIS-message, following the generated shortest path, in such a way that the timing of the generated messages are in agreement with the path distance and the vessel speed.

This approach also facilitates the use of harbour arrival and departure data as input values to the model, further improving the geographical coverage of ship activity tracking in cases of incomplete AIS coverage.

2.3 Evaluation of the influence of emission control areas, scrubbers and dual fuels

We have taken into account the influences of all internationally regulated emission control areas that were effective in 2015; these affect the maximum allowed Fuel Sulphur Content (FSC). These emission control areas include the North American SECA (sulphur ECA) region, the North European SECA region and the EU region. These regions have been treated in the model mathematically as polygons, inside which there were a set of rules that all ships must comply. E.g., within the EU region the FSC of a passenger ship must not exceed 1.5 %. During berthing for more than two hours, the FSC must not exceed 0.1 %. However, if on-board emission abatement systems are used, fuels with a higher FSC can be used but the effective emissions of $PM_{2.5}$ and SO_x must not exceed the corresponding emissions achieved by using the maximum allowed FSC without on-board emission abatement.

We have compiled a global up-to-date list of ships, which have a sulphur scrubber installed using publicly available data sources. The use of the scrubber together with the FSC regulations will determine dynamically the modelled FSC for individual ships (Johansson et al, 2013). We have assumed that the cheapest fuel is used that satisfies the regulations, allowing for the

technical limitations. Additionally, for open-loop scrubbers we have taken into account the additional power (2-3 %) required to operate the scrubber system. Whenever relevant, other emission abatement factors and technologies that affect emissions are also applied (Jalkanen et al, 2012).

The use of dual fuel engines that apply liquid natural gas (LNG) have also been implemented in the model. In case of the vessels equipped with such dual fuel engines, the fuel for the main engine is assumed to be switched to LNG during cruising mode. This affects the emission factors for CO_2, NO_x, $PM_{2.5}$ and SO_x.

3. Results

The global fuel consumption and the emissions were computed in a numerical grid using the WGS84 coordinate system. The grid contains 6,000 and 2,500 cells in each direction, respectively. This corresponds to a grid spacing of approximately 7 km in the vicinity of the equator.

3.1 Comparison of results with those of previous studies

We have compared the predicted consumption of fuel for the global shipping with the values reported by the International Energy Agency (IEA) and the predictions in the 3rd IMO greenhouse gas (GHG) study (Smith et al., 2015). This comparison is presented in Table 1, both for the total fuel consumption and for two marine fuel classes. However, the corresponding values for 2015 were not available in the above mentioned references; we have therefore included the latest reported values in the table. The known discrepancies of the presented IEA fuel statistics (export versus import discrepancy) have been discussed in (Smith et al., 2015); the presented IEA fuel statistics can be regarded as the lower limit, top-down estimates for the global fuel consumption.

Table 1: The predicted consumption of fuel for global shipping, reported by the International Energy Agency (IEA) and the 3rd IMO greenhouse gas study, compared with the values in this study. Notation: HFO is heavy fuel oil and MDO is mostly marine diesel oil, but also includes marine gas oil (MGO).

		IEA 2007 Statistics	**IEA 2011 statistics**	**IMO GHG3 2012 modelled**	**STEAM3 2015 modelled**
Total fuel consumption [10^9 kg]		249	254	300	276
	HFO	195	191	-	195
	MDO	54	62	-	81
Processed AIS-messages		-	-	3,700 10^6	7,800 10^6

Clearly, the fuel consumption values for different years are not quantitatively comparable. The total fuel consumption for 2015 evaluated in this study is 8.6 % larger than the corresponding value in 2011 by IEA, and 8.0 % smaller than the corresponding value by IMO GHG study for 2012. However, in the Third IMO GHG study it was assumed that weather effects alone would be responsible for 15% additional power requirement on top of the theoretical resistance requirements while in this work we have chosen not to implement such a scaling factor to the power requirements. Assuming that the modelled fuel consumption of STEAM3 would be correct, the difference between IEA 2011 and the value of this study in 2015 would indicate an annual growth of 2.1% for the fuel consumption of the global fleet between 2011 and 2015. Projections made by UNCTAD (Hoffmann et al., 2015) predicted an increase of 3.9% in seaborne trade for the above mentioned period; however, the increase in time of the fuel

consumption is expected to be smaller than that of seaborne trade, as there have been improvements in the energy efficiency of vessels and changes in the ship size.

The values evaluated separately for the two marine fuel classes are also not substantially different, as evaluated in this study in 2015, compared with those by IEA in 2011. Our modelled share of the use of the MDO fuel compared with the total fuel consumption is larger than the corresponding share of the use of the MDO fuel in the IEA statistics. This difference can be explained by the addition of new emission control areas, or stronger regulations in existing emission control areas, during 2011 and 2015. For example, in the Northern European ECA the use of the HFO fuel was generally not possible in 2015, without the use of emission abatement equipment. We conclude that the predictions of the present study for the fuel consumption are not in a disagreement with these two previous studies.

We have also evaluated the global amount of marine trade. This was computed based on the distances sailed and the cargo capacity of vessels, according to the principles of the use of cargo space, as defined in the 2nd IMO GHG study (Buhaug et al., 2009). The world seaborne trade was estimated to be 103,000 billion (10^9) ton km. This value is not substantially different from the estimate by UNCTAD (Hoffmann et al., 2015) of 100,447 billion ton km for 2015 (converted from 54,237 billion ton miles). The difference between these two estimated values is less than 3 %.

3.2 The globally summed annual emissions from shipping

The total annual emissions estimated in this study are presented in Table 2. The IMO-registered marine traffic is responsible for most of the emissions for all the considered pollutants, e.g., for approximately 91 % and 93 % of the CO_2 and $PM_{2.5}$ emissions, respectively. However, the presented emission totals are likely to underestimate the global shipping emissions as the weather effects were not taken into account in this study. Additionally, the lack of AIS-data in some coastal regions can also contribute to this underestimation, for which an example exists: previously, using 1.7 billion terrestrial AIS-messages at the Baltic Sea the authors estimated the annual CO_2 emissions at the Baltic Sea to equal 15,900 kton (Gg) in 2015 (Johansson and Jalkanen, 2016). In this study the total amount of AIS-messages in the same area was only 61 million and the modelled CO_2 emissions was approximately 7% less, 15,000 kton.

Table 2: Predicted annual emissions, distances travelled, payloads and the numbers of ships in this study for 2015. The values have been separately presented for all ships, for IMO registered ships, the ships that have been identified using their MMSI values, and for ships that have not been identified.

		NO_x [10^6 kg]	SO_x [10^6 kg]	$PM_{2.5}$ [10^6 kg]	CO [10^6 kg]	CO_2 [10^6 kg]	Travel [10^6 km]	Payload [10^9 km*ton]	Ships
All ships		20,880	9,690	1,490	1,350	831,300	5,050	105,490	376,219
	IMO-registered	19,200	9,180	1,390	1,220	756,000	3,630	101,860	65,804
	Identified, non-IMO	1,560	487	88	115	69,000	1,240	3,630	234,438
	Not identified	124	24	6	13	6,800	180	-	75,977

The number of non-IMO registered vessels, approximately 311,000, is substantial. Especially for the non-IMO registered vessels the technical data assimilation methods presented in this paper have been in a key role and in 234,438 cases the technical data assimilation method provided a concrete result; in such cases the basic physical properties of the ships were identified and the missing technical details were then provided by the MSV-data assimilation method. Respectively, there were approximately 76,000 vessels, for which the technical data assimilation methods did

not yield enough information for vessel characterization. For such vessels, the ships were assumed to be generic small boats with a gross tonnage of 300 t (Johansson et al., 2013). However, only 3.5 % of all travel kilometres were travelled by these unknown vessels. As the total distance travelled by such crafts is relatively small, the resulting uncertainty caused to the global emission budget is also fairly small.

The use of the route generation algorithm was limited for approximately 9% of the total travel distances and the generated routes were clearly concentrated on the Middle East and Asia. In a separate model run, disabling the use of the route generation algorithm (Appendix B) in these two regions, the modelled shipping emissions frequently occurred over the land areas in the Middle East, China, Malaysia and Vietnam. Without the use of route generation the land-crossing route segments were often not modelled at all since the distance, duration and vessel speed information were at odds with each other. In such cases the filtering algorithms (Johansson et al. 2013) prevented the modelling of these infeasible route segments.

The CO_2 emissions from global shipping were classified according to the flag state, which was determined based on the Marine Information Digits (MID; the first three numbers of the MMSI code). The four largest fleets (Panama, China, Liberia and Marshall Islands) were responsible for almost a half (48.4%) of the total CO_2 emissions in 2015 (832 million tons). The fleets from fifth to eighth (Singapore, the United Kingdom, Malta and Bahamas) were responsible for 20 % of the emissions. However, the largest four fleets carried 57 % of the global seaborne cargo; this value is larger than their corresponding share of the global CO_2 emissions from shipping.

3.3 Geographical distribution of the global emissions from shipping

The geographical distributions of the annual emissions of $PM_{2.5}$ and SO_x in 2015 have been presented in Figs. 3 – 4. The names of the sea areas, as referred to in this article, have been presented in Supplements B. The modelling has been done for latitudes from 80° S to 80° N; shipping in the remaining Antarctic and Arctic regions is negligible.

Broadly speaking, the highest emissions of both $PM_{2.5}$ and SO_x per unit area occur in the Eastern and Southern China Seas, in the sea areas in the south-eastern and southern Asia, in the Red Sea, in the Mediterranean, in North Atlantic near the European coast, in the Gulf of Mexico and the Caribbean Sea, and along the western coast of North America.

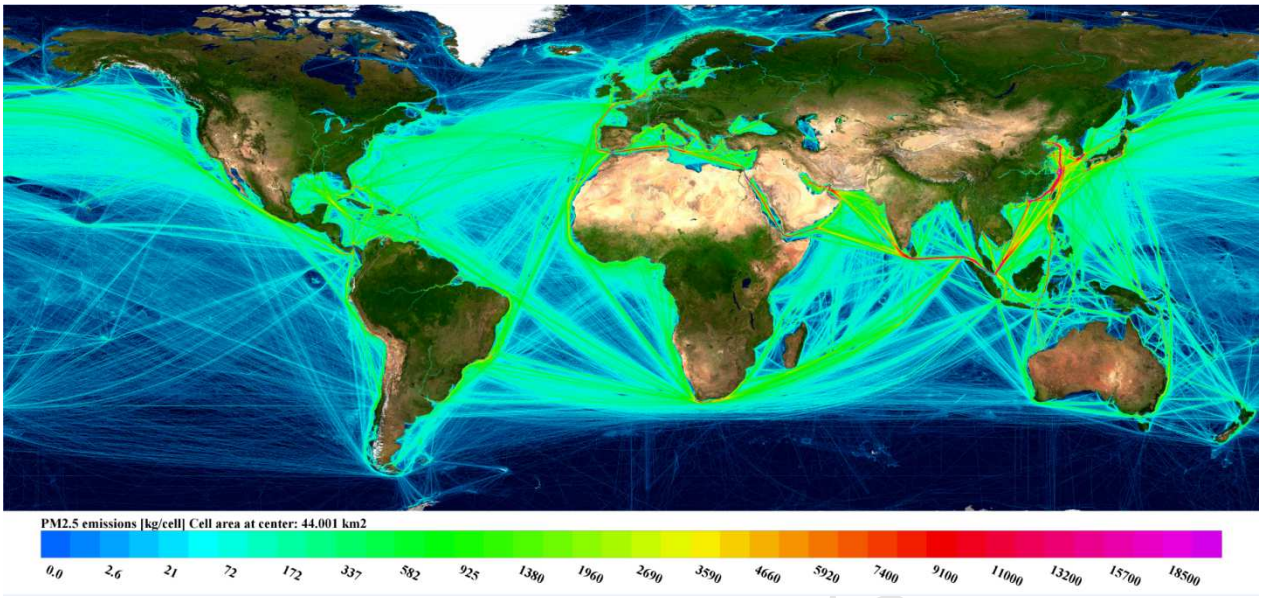

Figure 3: Geographical distribution of the modelled total $PM_{2.5}$ emissions from shipping in 2015. - Background satellite imagery provided by NASA Earth Observatory. The legend refers to the emission divided by the area of each numerical grid cell (in units of kg km^{-2}).

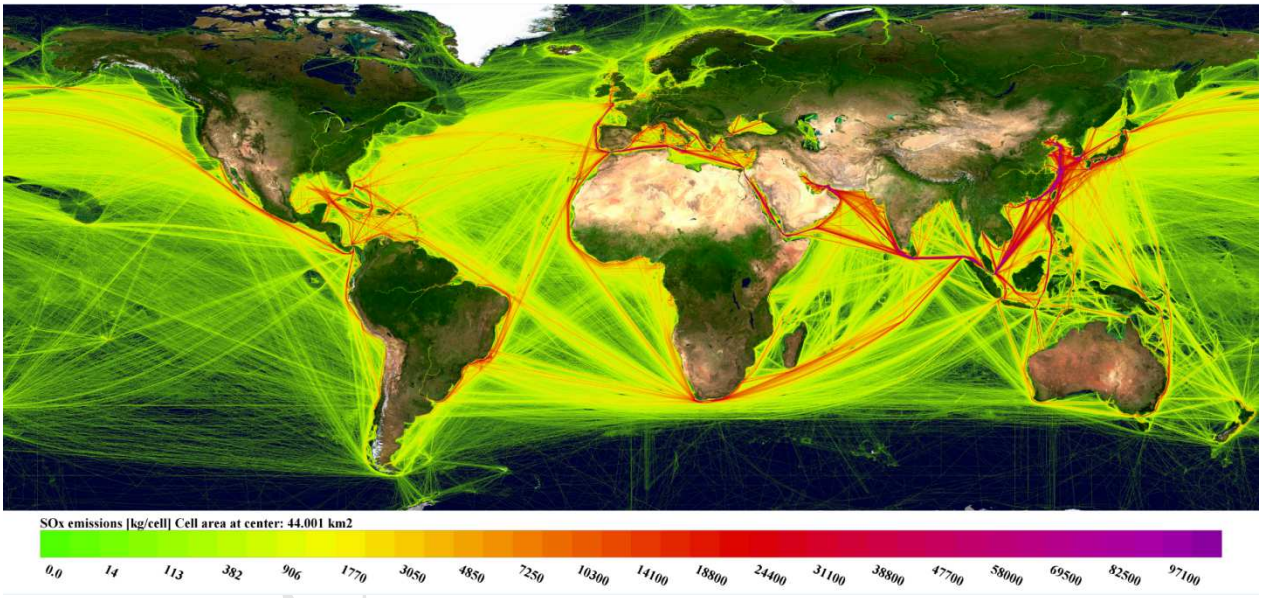

Figure 4: Geographical distribution of modelled total SO_x emissions from shipping in 2015.

An additional detailed geographical analysis shows that the highest emission densities in a decreasing order, as measured within a circle of 10 kilometres, occur in Singapore, Hong Kong, Antwerp, Shanghai, Los Angeles and Rotterdam. In the geographical distribution of SO_x emissions from shipping (Fig. 4), the effects of the SECA regions are visible along the coastlines of northern America, in the Gulf of Mexico, in the North Sea and in the Baltic Sea.

3.4 The shipping emissions for the sea regions and the size categories of ships

The emissions of three main pollutants from global shipping have been presented separately for the main sea regions in Fig. 5. Additionally, the NO_x emission density in these regions was chosen and has been presented in the figure. These selected geographic areas have been described in greater detail in Supplements B.

Regarding the overall total emissions of the sea regions, the highest emissions occurred in the North Atlantic, North Pacific, South China Sea, Indian Ocean and South Atlantic. Geographically, the largest oceans are the South Pacific, North Atlantic and Indian Ocean. Considering the emission densities of these sea regions, the Singapore Strait by far has the highest emission density for all modelled pollutants. Also the Malacca Strait, the Eastern China Sea and the Yellow sea have high emission densities, also for other pollutant types than NO_x. The ECAs are clearly visible as they have low SO_x and $PM_{2.5}$ emissions with respect to the relative NO_x emissions. Based on the emission totals of the present study, the global average of marine fuel sulphur content of IMO registered traffic was 1.9% (by mass) in 2015, but there are significant regional differences caused by various sulphur regulations.

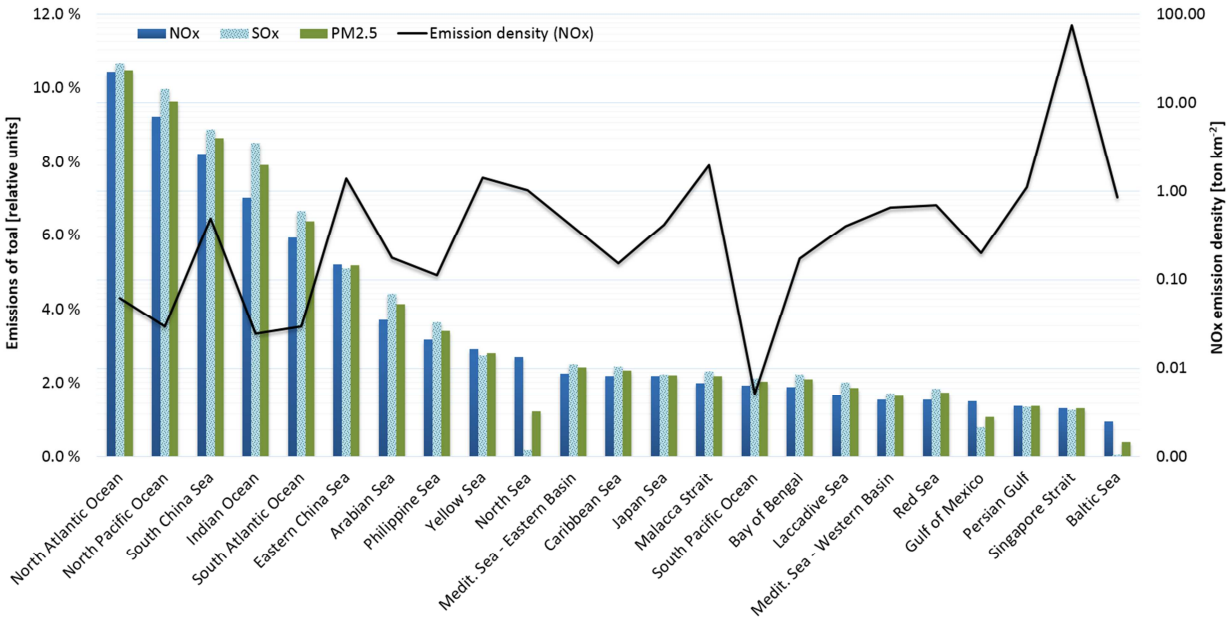

Figure 5: Relative share of the emissions of NO_x, SO_x and $PM_{2.5}$ from the total global shipping emissions (bar graph). The emission density for NO_x emissions are presented with a black line using a logarithmic scale.

The numbers of ships, their cargo transport work and their emissions have been presented in Fig. 6, separately for the size classes of ships. For instance, there were 4,508 ships globally that had a gross tonnage (GT) larger than 80,000 tons; this constitutes 6.8 % of all IMO-registered vessels. Despite the low amount of ships, however, their contribution to the global shipping emissions for the four considered pollutants ranged from 28 to 33 %. These large vessels also carried 43.7 % of all transported marine cargo.

The lowest size category (below 4,000 tons) contains 88.5% of all ships. However, despite the large numbers of the smallest vessels, the two categories of smallest ships (below 10,000 tons) are responsible for the smallest shares of the emissions of $PM_{2.5}$ and SO_x. The minor contribution of emissions originating from the smallest vessel size category can be explained by the combination of low average travel amounts (5000km per ship on average) and low-powered engines on board, which in turn operate on heavy fuels less often than the vessels in other size categories.

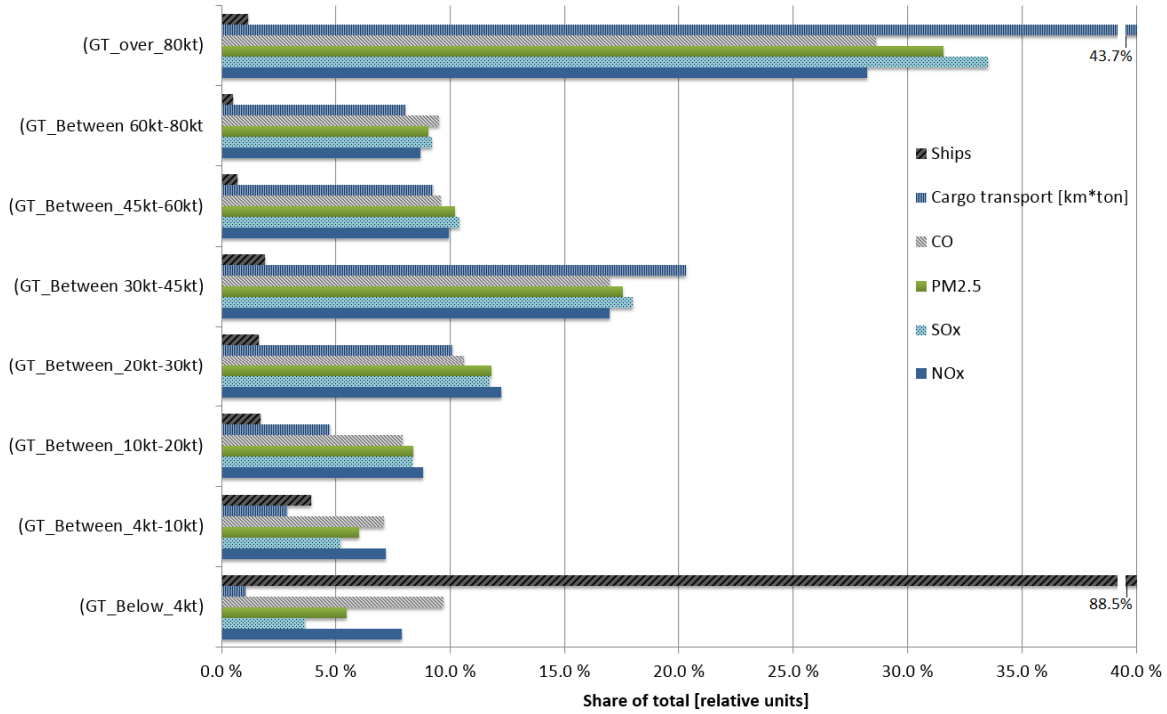

Figure 6: The numbers of ships, transport work (payload; km * ton) and the shares of global total emissions for four pollutants in 2015, classified in terms of the size categories of ships (measured as gross tonnage, GT).

3.5 Emissions for various ship types

The responsibilities of various ship categories for the global CO_2 emissions in 2015 have been presented in Fig. 7. The most significant contributions were from container ships, cargo carriers and tankers; their combined CO_2 emissions were 82.6 % of the total emissions of the global fleet. Regarding the other pollutants considered in this study, the relative global share of these major ship categories is larger than 80 %. The above mentioned three ship types contribute 84, 88 and 87 % of the global NO_x, SO_x and $PM_{2.5}$ emissions, respectively.

Military ships that send AIS-messages have been included in the modelling and they are a part of the "Miscellaneous" vessel category. However, only some auxiliary naval vessels (cargo ships, tankers etc.) carry AIS and use it; unfortunately, the activities of destroyers, frigates and other battle ships which may have unit emissions equal to those of container vessels (Corbett and Koehler, 2003) cannot be accurately described using AIS data.

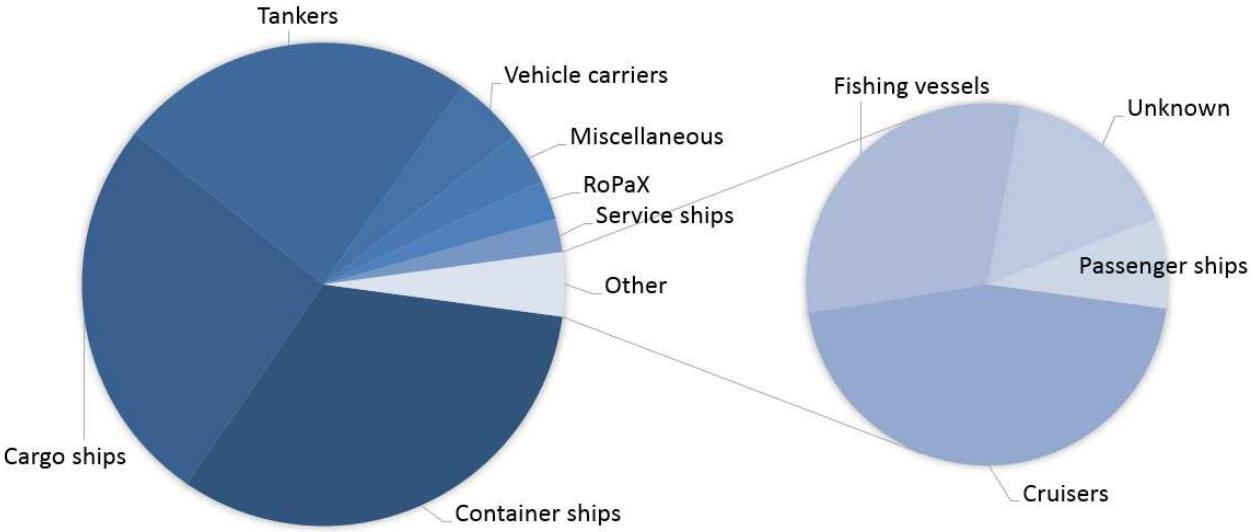

Figure 7: Shares of global CO_2 emissions for various ship categories in 2015. Vehicle carriers include the RoRo vessels. The category called miscellaneous includes tugs, dredgers, barges, search and rescue, ice breakers, law enforcement and some military vessels. Cargo ships include bulk carries and general cargo vessels.

The spatial distribution of the CO_2 emissions has been separately presented in Figs. 8a-f for six vessel categories. There are substantial differences between these distributions, in terms of the ship type. In particular, the spatial distributions for the cargo transport (Figs. 8a-b) are clearly different from those of passenger traffic (Fig. 8d, partly also 8c). The RoPax traffic consists mainly of fairly short routes in the vicinity of coastlines. The disaggregation of emissions to vessel type specific contributions facilitates further work with sophisticated scenarios as future fleet growth -rates are not the same for all ship types.

There is no intensive tanker traffic from the Persian Gulf to USA, which can be partly caused by the increased domestic oil production in the USA (US EIA, 2017; (Hoffmann et al., 2015)). Regarding the cruiser traffic, Hawaii and Tahiti are significant hubs of traffic in the Pacific; other hotspots are Miami, Cancun, Seychelles and Mauritius. As expected, the geographical distribution of fishing boats is more dispersed than those for the other ship categories. The amount of fishing traffic may be underestimated, as part of the fishing boats may not use the AIS equipment.

On average, shipping can produce low specific emissions per cargo ton kilometre. The computed average of specific CO_2 emissions was 7.6 grams per ton (of cargo) km for all ships, but there is a wide variety between different kinds of ships. According to this study, in terms of cargo transport work, bulk cargo carriers and oil tankers had the smallest specific emissions of 4.7 and 6.1 grams per ton km. Containerships emitted 9.7 and RoRo/RoPax ships 150.7 grams per ton km. However, the specific emission value (per ton of cargo) for RoRo/RoPax ships is not directly comparable, as this category includes ships, which carry both passengers and cargo. In the above mentioned specific emission calculation, only the mass of cargo was considered instead of the combined mass of cargo and passengers; this tends to result in an overestimation in specific emissions for passenger vessels. In summary, there is a wide variation of the specific emissions for the different types of ships; some ship types may have specific emissions that are similar to those of passenger cars (EEA, 2017). The specific emissions can also vary significantly for the

range of ships within any specific ship category, depending, e.g., on the design speeds and the age of the vessels.

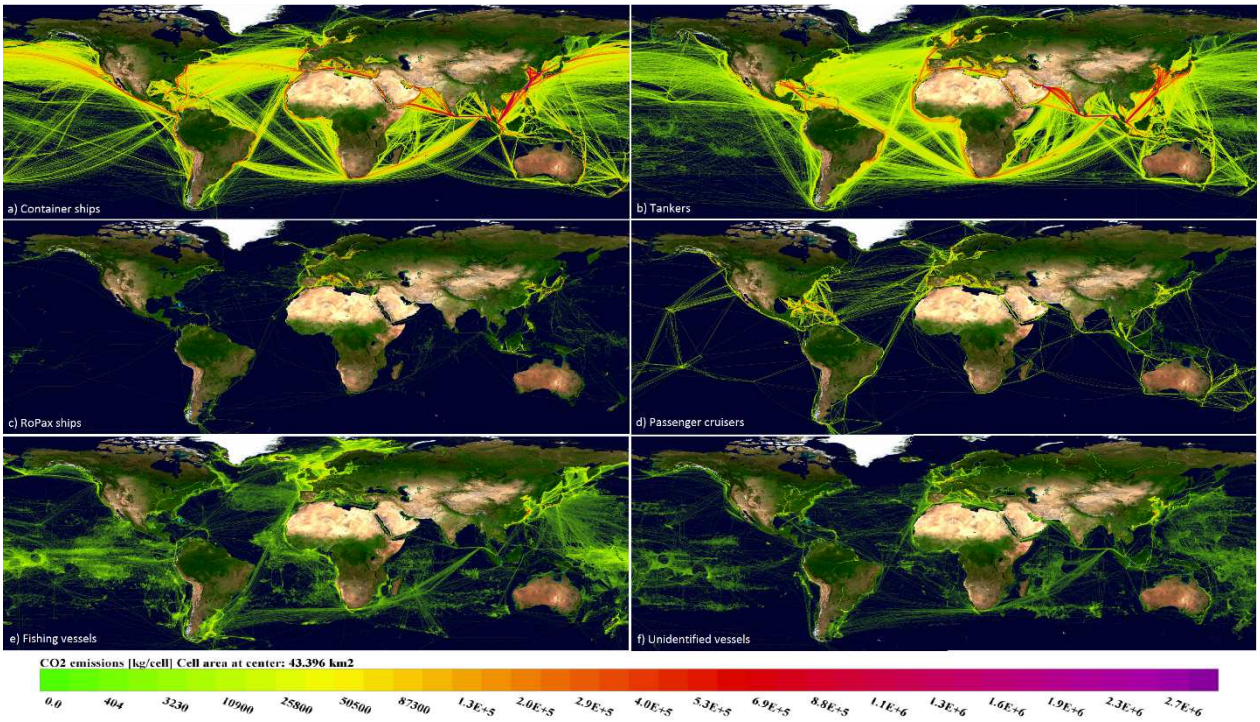

Figure 8a-f: Global distribution of the CO_2 emissions for selected ship types and unidentified vessels in 2015. a) Container ships, b) tankers, c) RoPax ships, d) Passenger cruisers, e) fishing vessels and f) unidentified vessels.

4. Conclusions

We have presented a comprehensive global shipping emission inventory for 2015. The emissions were evaluated using the STEAM3 model, with input data from the Automatic Identification System and the vessel specification database. The emission model was improved in several respects in this study. Previously, there have been two major obstacles in assessing accurately global shipping emissions. The first one is that the required technical specifications of ships are incomplete or missing in some cases. We have therefore developed a method for the collection and processing of the technical ship data, using data assimilation techniques. We included in this modelling approximately 300,000 vessels with unique technical characteristics, given by the technical data assimilation methods. After using this procedure, only 3.5% of the total travel kilometres were estimated to be travelled by vessels with unknown characteristics. We have therefore managed to evaluate the emissions of non-IMO registered marine traffic substantially more accurately, compared with previous corresponding investigations.

It has also been challenging to evaluate accurately global shipping emissions, as the AIS-data can be notably heterogeneous, and it is therefore difficult to realistically determine the shipping activities. We have developed a model that applies shipping route generation algorithms that automatically refines the ships' travel routes whenever the spatial and temporal gap between two consecutive AIS-messages is so large that it suggest a need for a more detailed approach. During the target year 2015 the route generation feature was found to be especially beneficial in the regions of Middle East and Asia. As we methodically evaluate the shipping activities between the AIS-messages, the heterogeneity and reliability of the AIS-data (e.g., duplicate messages and

erroneous information) will not significantly affect the outcome of the modelling results. The inclusion of the route generation algorithm also allows the use of additional ship activity datasets, such as the information on arrival and departure times to harbours. This can improve the coverage of the shipping activity datasets in open-sea regions, in which the AIS coverage may be incomplete.

The number of AIS messages used in this study was approximately eight billion (7.8×10^9), which was significantly larger than, e.g., the corresponding value used for the results in the 3rd IMO GHG. The number of satellite AIS transceivers in orbit around the Earth has increased during the last few years, and this trend is expected to continue in the future. This trend is fortunate since there are no restrictions for the size of the activity dataset in STEAM3. Better availability of the AIS data has provided, and will provide, better possibilities for more accurate predictions of the shipping emissions. Having larger amount of AIS data is especially beneficial for the modelling of coastal regions with significant amount of short-sea shipping, in which case the route regeneration algorithm is unable to recover the missing route information in most cases.

The predictions of the STEAM3 model have previously been extensively evaluated against experimental measurements (e.g., Jalkanen et al., 2009; Jalkanen et al. 2012; Johansson et al., 2013; Berg et al., 2012; Beecken et al., 2014). In this study we did not conduct an evaluation of the numerical results against experimental data. Such an evaluation on a global scale would require the use of a dispersion model in combination with the emission model, and an analysis of the relevant satellite and ground-based data. However, the computed global results were compared with (i) those in the third Greenhouse Gas Study of the International Maritime Organisation, and (ii) those reported by the International Energy Agency. However, it was not possible to inter-compare the results quantitatively, as both the IMO and the IEA studies have evaluated their results only for earlier years, viz. 2012 and 2011, respectively. However, allowing for the moderately increasing trends of the global marine traffic in the early 2010's, the results of this study for the fuel consumptions can be considered to be qualitatively in agreement with the results presented in both of the above mentioned studies. The inclusion of environmental factors that can increase the fuel consumption of ships, such as the waves, wind, ice coverage and sea currents, would bring the bottom-up fuel consumption estimates produced with the model even closer to the top-down fuel statistics.

We conclude that it is possible to analyse the global shipping activities using the AIS signals of individual ships, combined with modelling, to obtain results that are in agreement with the reported top-down fuel statistics. It is expected that the IMO Data Collection System and EU Monitoring, Reporting and Verification systems (EU, 2015) will in the future provide a good benchmark for fuel consumption modelling of the global fleet in the future. Both of these systems make fuel consumption reporting mandatory on ship level.

The global geographical distribution was presented for the annual emissions of $PM_{2.5}$ and SO_x in 2015. The highest emissions per unit area occurred in the following sea regions: Eastern and Southern China Seas, in the sea areas in the south-eastern and southern Asia, in the Red Sea, in the Mediterranean, in North Atlantic near the European coast, in the Gulf of Mexico and the Caribbean Sea, and along the western coast of North America. We also considered emission hotspots, by evaluating the highest emission densities within limited areas. We defined those as areas within a circle of 10 kilometres, and found the highest emissions to occur, in a decreasing order, in Singapore, Hong Kong, Antwerp, Shanghai, Los Angeles and Rotterdam.

The use of the STEAM3 model makes it possible to analyse the emission results in a detailed and versatile manner. In this study, we have analysed the global emissions of various pollutants in terms of the sizes of ships, the flag states and the ship categories. The global spatial distributions of emissions are substantially different for the various ship types. For instance, the spatial distributions for the cargo transport are clearly different from those of passenger traffic.

The results of this study can be used in air quality modelling on scales from local to global. One possible application could be an evaluation of the health effects caused by global shipping emissions to the atmosphere. The STEAM3 model can also be used to provide more detailed emission data from shipping, for instance, for a selected set of harbours or some other limited area, using a selected temporal and spatial resolution. Annual updates to global ship emission inventories can also be provided with the model, if an access to the global AIS datasets will be available. The presented global emission inventory, in combination with the STEAM3 model or some other modelling system, could in the future also be used to assess the impacts of various emission scenarios. Such scenario simulations can be performed with the model since the effective regulations, physical properties of ships and even the travelling speed of ships can be made variable.

5. Appendices

Appendix A: Technical data assimilation

The performance of the technical data-assimilation method presented in the paper was evaluated. For randomly selected database entries the assimilation method was used to estimate main engine power, auxiliary engine power, gross tonnage (GT) and the main engine stroke type using the MSV search method described in Section 2.1. The estimates were then compared against the actual values listed in the database entries and for the selected vessel properties the Root Mean Squared Error (RMSE) were calculated. Over 3,000 database entries was included; perfect matches were not allowed to occur in the evaluation (i.e., the data for assimilation always originated from a different database entry. Simply put, the Most Similar Ship was not allowed to be the evaluated ship itself).

For the assignment of the weighting factor a in Eq. 1 the evaluation process was repeated with variable values for the factor a. The lowest RMSE value for the main engine estimates (which is the most crucial technical piece of information for the modelling) was achieved by assigning the value of 0.35 for the factor a. Importantly, by setting the factor a equal to zero significantly increased the achieved RMSE which clearly indicates that a two-dimensional search criterion is better than a simpler one-dimensional length criterion.

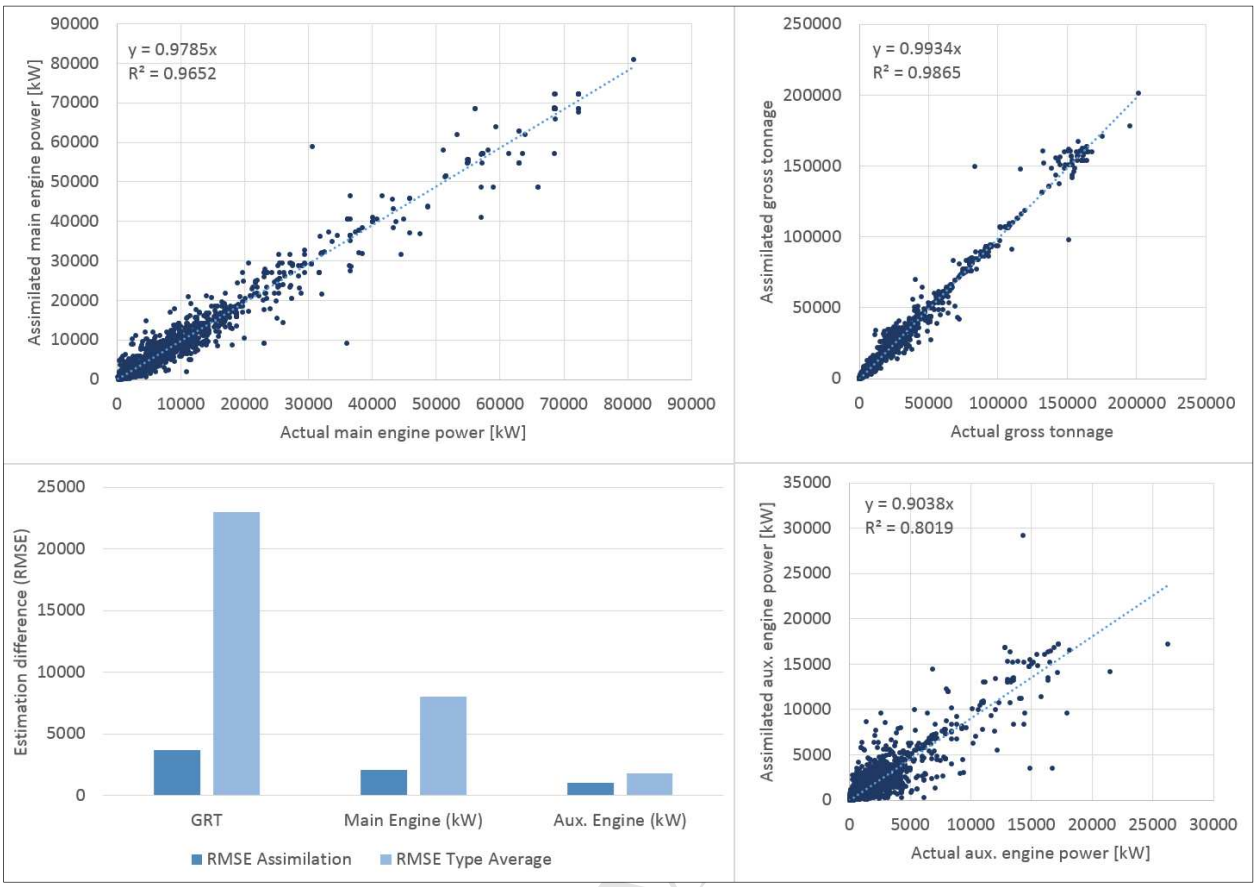

Figure A1a-d: Selected evaluation results for the technical data-assimilation method used in the STEAM3 model.

Figure A1 describes the results for the evaluation study. The assimilated gross tonnage and main engine power are in good agreement; the assimilated auxiliary engine has the highest variability with respect to actual database values and the correlation coefficient R^2 is 0.8. The stroke type for the main engine was correctly assimilated in 89% of the evaluation cases.

The main argument for the use of the technical data-assimilation method is that using vessel type averages for missing technical pieces of information can be detrimental for shipping emissions modelling. Average values for missing data may easily lead to unrealistic description in hydrodynamic performance prediction, fuel consumption and emissions. In the evaluation we calculated RMSE values when vessel type -based averages were used instead. We generated the vessel type averages based on our full vessel database. According to our results by using vessel type averages the RMSE for gross tonnage assignment is approximately 6 times the RMSE achieved with the data-assimilation method. Respectively, the RMSE for main engine power is approximately 4 times larger and the RMSE for aux. engine power is 80% larger.

As described above the technical data-assimilation method relies on the design speed of the vessel for which the method is being used (note: the method can still be used when the scaling factor a is set to 0). However, the design speed is not always available and for ships without IMO-number the design speed is in fact almost always missing. In such cases the design speed is estimated based on AIS-data. The instantaneous speed values given by the AIS-data are sorted in order of magnitude. Based statistical regression we then estimate the design speed of the vessel to equal the 95^{th} percentile value of the ordered speed data multiplied by a factor of 1.05. The main reason for using the percentiles in the evaluation is that the simple maximum value for the instantaneous speed correlates with the design speed significantly worse (Figure A2), because of

630 erroneous data and external phenomena like sea currents that can influence on speed entries of
631 AIS.
632

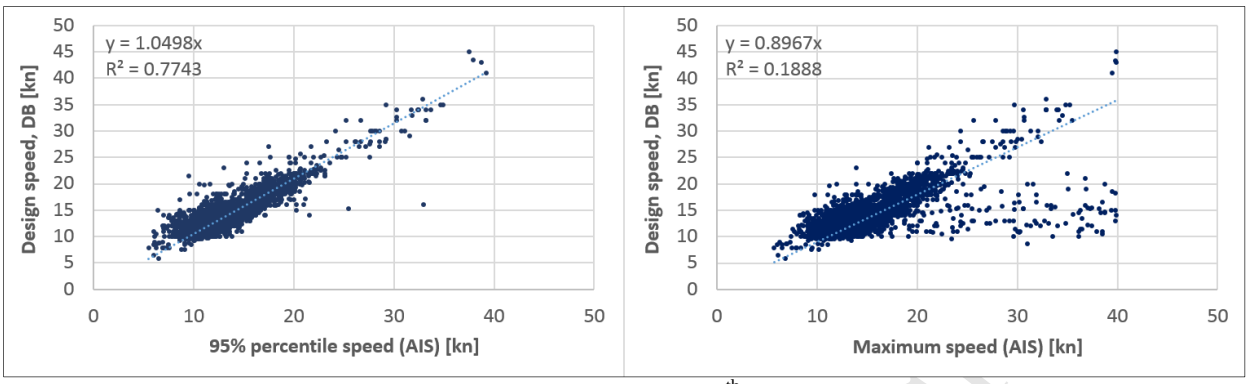

633
634 Figure A2a-b: The correlation of design speed versus the 95th percentile speed (a) given by AIS and the
635 maximum instantaneous speed given by AIS (b). The used sample included more than 3,000 IMO-
636 registered ships during 2015.

637

Appendix B: Shortest path route generation algorithm

If two consecutive AIS position reports indicate a significant geographical difference and a land mass in between the two known points exists, a Dijkstra algorithm is used to determine the shortest path network (Cherkassky et al, 1996) between two arbitrary marine locations. The basis for the algorithm is the network of nodes and arcs that facilitates the use of shortest path network algorithm.

The network of nodes are constructed based on existing global STEAM3 model run using the gridded fuel consumption data (7km grid cell resolution near the equator) for IMO-registered vessels. The resulting visual representation of the fuel consumption was converted into a Google Earth layer. For each major shipping route visible within the layer several hundred lines were drawn in the locations of the visible shipping routes. The numerical values of the line coordinates were then stored and saved in a kmz-file.

The route generation module has a conversion tool which transforms the collection of Google Earth lines into an inter-connected network of nodes and arcs, which the network algorithm operates on. Basically, all coordinate points in each line are converted into nodes and consecutive nodes are connected with two parallel arcs with opposite directions. In cases where two or more lines cross, the conversion tool places an additional node at the intersection and connects the intersecting lines with additional arcs.

Label setting methods for solving the shortest path problem

For the shortest path generation a 'label setting method' is used, first published by Dijkstra in 1959. The algorithm iterates as follows:

> **Step 0 - initiation:** Each node n_i is associated with a label d_i, which in this particular case can be directly associated as the minimum travel distance to the node n_i. Initially all labels are set to infinity and updates as the algorithm is being iterated.
> A candidate list V of nodes to be evaluated in the following iterations is formed. The start node n_s (which is the closest node from the ship's initial position) is added to the candidate list and the label of the node is set to 0.
>
> **Step 1 – candidate selection:** The node i with the lowest label is removed from the candidate list.
> **Step 2 – label setting and new candidates identification:** For each arc (i, j) associated with the removed candidate node i, if $d_j > d_i + a_{ij}$, we set $d_j = d_i + a_{ij}$ and node j is added to V if it does not already belong to V. The node i is also listed as the "predecessor" node for the node j.
> **Step 3 - termination:** If the candidate list V is empty or the removed candidate node i is the node closest to the ship's end destination, the algorithm terminates. Otherwise, steps 1-3 are repeated.

Eventually the algorithm terminates and then the sequence of nodes leading from the start node to the end node (i.e., the short path) can be extracted by following the list of the predecessor nodes. The physical travel distance between the start and end points is also available, and is given by the end-node's label value. The sequence of travel points is then converted into proxy AIS-messages for the model. The traveling speed for the generated route can be adjusted to reflect the distance and temporal separation in case the average speed between the start- and end-point activity data is assessed to be infeasible (this can happen e.g., if the ship is initially berthing). Afterwards the

cruising speed correction, proper timestamps are associated with each generated travel point. In case the travel distance and travel time is clearly impossible for the ship (e.g., the adjusted travel speed significantly exceeds the design speed of the ship) then generated route is discarded and not modelled.

Algorithm performance

In general, a shortest path algorithm is computationally heavy operation. The computational task for solving the shortest path problem increases exponentially when the number of nodes and arcs are increased. As a solution, all the shortest path routes (approx. 12 million unique routes) has been computed before-hand and the stored shortest path routes can be accessed without significant computational effort. This has been done as follows:

- By ignoring the Step 3 end clause when the end node is removed from the candidate list, the algorithm finishes and has generated the shortest path (the predecessor node sequences) for each other node in the network.
- The algorithm is run once for each of the node in the network (approx. 5,000 times). All the resulting predecessor lists are stored to easy access look-up tables.
- During model run, for any location the nearest node is searched and the pre-calculated predecessor lists are used to assess the shortest path to any other location without significant computational effort.

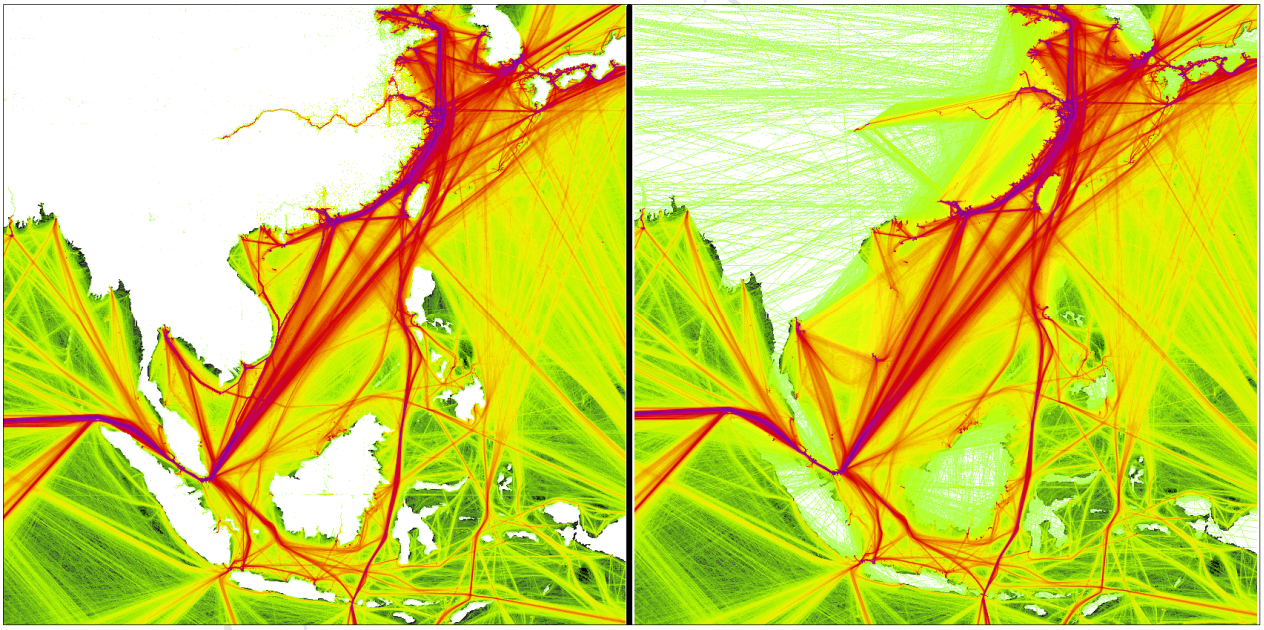

Figure B1a-b: Modelled annual total shipping emissions (CO_2) with and without the route generation algorithm. Left in (a), the modelled emissions, as presented in the paper, are indicatively illustrated in a selected area in Asia. Right in (b), the modelled emissions are shown when the route generation algorithm has been disabled in a separate model run.

The importance of the route generation algorithm in global shipping emission assessment is highlighted in Figure B1. A separate model run was performed without the route generation algorithm and the resulting geographical distribution of modelled emissions were compared against the gridded emissions presented in the paper. The differences were clearly visible especially in Asia. Without the route generation algorithm, significant portion of the shipping activities and thereby emissions would incorrectly occur inland.

6. Author contribution

L. Johansson designed and carried out the technical model development described in the paper and processed the input data required for the shipping emissions modelling. He is also responsible for the shipping emissions modelling work, evaluation studies and figures presented in the paper. He prepared the manuscript with contributions from all co-authors.

J.-P. Jalkanen was responsible for acquisition of AIS-data and technical vessel database. He assisted in the model development work, assisted the manuscript preparation and was responsible for the literature review and comparisons against recent literature.

J. Kukkonen contributed in the literature review, and the preparation and writing of this manuscript.

7. Acknowledgements

This study has been a part of the research projects EPITOME (Project KOL-1601: Emissions from ship and the impacts on human health and environment - now and in the future) and NordicWelfAir (Project #75007: Understanding the link between Air pollution and Distribution of related Health Impacts and Welfare in the Nordic countries).

8. References

Aulinger, A., Matthias, V., Zeretzke, M., Bieser, J., Quante, M. and Backes, A.: The impact of shipping emissions on air pollution in the greater North Sea region - Part 1: Current emissions and concentrations, Atmos. Chem. Phys., 16(2), 739–758, doi:10.5194/acp-16-739-2016, 2016.

Beecken, J., Mellqvist, J., Salo, K., Ekholm, J. and Jalkanen, J.-P.: Airborne emission measurements of SO2, NO2 and particles from individual ships using a sniffer technique, Atmos. Meas. Tech., 7(7), doi:10.5194/amt-7-1957-2014, 2014.

Berg, N., Mellqvist, J., Jalkanen, J.-P. and Balzani, J.: Ship emissions of SO 2 and NO 2: DOAS measurements from airborne platforms, Atmos. Meas. Tech., 5(5), doi:10.5194/amt-5-1085-2012, 2012.

Buhaug, Ø., Corbett, J. ., Endresen, Ø., Eyring, V., Faber, J., Hanayama, S., Lee, D. ., Lee, D., Lindstad, H., Markowska, A. ., Mjelde, A., Nelissen, D., Nilsen, J., Pålsson, C., Winebrake, J. ., Wu, W. and Yoshida, K.: Second IMO GHG Study2009, Int. Marit. Organ., 240, doi:10.1163/187529988X00184, 2009.

Cherkassky, B. V., Goldberg, A. V., and Radzik, T. Shortest paths algorithms: Theory and experimental evaluation. Mathematical programming, 73(2), 129-174, 1996

Corbett, J. J., Winebrake, J. J., Green, E. H., Kasibhatla, P., Eyring, V., and Lauer, A.: Mortality from ship emissions: a global assessment, Environ. Sci. Technol., 41, 8512–8518, doi:10.1021/es071686z, 2007.

Corbett, J. J., and H. W. Koehler, Updated emissions from ocean shipping, J. Geophys. Res., 108(D20), 4650, doi:10.1029/ 2003JD003751, 2003.

European Union, Regulation 2015/757 of the European Union and of the Council on the monitoring, reporting and verification of carbon dioxide emissions from maritime transport, 2015

European Environmental Agency, Energy Efficiency and specific CO_2 emissions, Indicator Assessment IND-110-en, 2017, http://www.eea.europa.eu/data-and-maps/indicators/energy-efficiency-and-specific-co2-emissions/energy-efficiency-and-specific-co2-9, last accessed March 20th 2017.

Goldsworthy, L. and Glodsworthy, B., Modelling of ship engine exhaust emissions in ports and extensive coastal waters based on terrestrial AIS data – An Australian case study, Environmental Modelling & Software, 63, 45-60, http://dx.doi.org/10.1016/j.envsoft.2014.09.009, 2015.

Hoffmann, J., Juan, W. and Miroux, A.: Developments in international seaborne trade, United Nations Publ., 1–28 [online] Available from: http://unctad.org/en/pages/PublicationWebflyer.aspx?publicationid=753, 2015.

Hollenbach, K. U.: Estimating resistance and propulsion for single screw and twin screw ships, Ship Technology Research, 45/2, 1998.

Jalkanen, J.-P., Brink, A., Kalli, J., Pettersson, H., Kukkonen, J. and Stipa, T.: A modelling system for the exhaust emissions of marine traffic and its application in the Baltic Sea area, Atmos. Chem. Phys., 9(23), 2009.

Jalkanen, J.-P., Johansson, L., Kukkonen, J., Brink, A., Kalli, J. and Stipa, T. Extension of an assessment model of ship traffic exhaust emissions for particulate matter and carbon monoxide. Atmos. Chem. Phys., 12, 2641–2659, 2012.

Jalkanen, J.-P., Johansson, L. and Kukkonen, J. A Comprehensive Inventory of the Ship Traffic Exhaust Emissions in the Baltic Sea from 2006 to 2009. Ambio, Volume 43, Issue 3 (2014), pp. 311-324, DOI 10.1007/s13280-013-0389-3, http://www.springerlink.com/openurl.asp?genre=article&id=doi:10.1007/s13280-013-0389-3, 2012.

Jalkanen, J.-P., Johansson, L., Kukkonen, K. A comprehensive inventory of ship traffic exhaust emissions in the European sea areas in 2011. Atmos. Chem. Phys., 16, 71–84, 2016. http://www.atmos-chem-phys.net/16/71/2016/acp-16-71-2016.pdf, 2016.

Johansson, L., Jalkanen, J-P., Kalli, J., and Kukkonen, J. The evolution of shipping emissions and the costs of recent and forthcoming emission regulations in the northern European emission control area. Atmos. Chem. Phys., 13, 11375–11389, www.atmos-chem-phys.net/13/11375/2013/, doi:10.5194/acp-13-11375-2013 doi:10.5194/acpd-13-16113-2013, 2013.

Johansson, L. and Jalkanen, J-P. Emissions from Baltic Sea shipping in 2015, HELCOM Baltic Sea Environment Fact Sheets, available from http://www.helcom.fi/baltic-sea-trends/environment-fact-sheets/maritime-activities/emissions-from-baltic-sea-shipping/, accessed October 10th 2017, 2016.

Jonson, J. E., Jalkanen, J. P., Johansson, L., Gauss, M. and Van Der Gon, H. A. C. D.: Model calculations of the effects of present and future emissions of air pollutants from shipping in the Baltic Sea and the North Sea, Atmos. Chem. Phys., 15(2), doi:10.5194/acp-15-783-2015, 2015.

Liu, H., Fu, M., Jin, X., Shang, Y., Shindell, D., Faluvegi G., Shindell, C. and He, K. Health and climate impacts of ocean-going vessels in East Asia. Nature Climate Change. 5 pp., DOI: 10.1038/NCLIMATE3083, 2016.

Marelle, L., Thomas, J. L., Raut, J.-C., Law, K. S., Jalkanen, J.-P., Johansson, L., Roiger, A., Schlager, H., Kim, J., Reiter, A., and Weinzierl, B.: Air quality and radiative impacts of Arctic shipping

emissions in the summertime in northern Norway: from the local to the regional scale, Atmos. Chem. Phys., 16, 2359-2379, doi:10.5194/acp-16-2359-2016, 2016.

Matthias, V., Aulinger, A., Backes, A., Bieser, J., Geyer, B., Quante, M. and Zeretzke, M.: The impact of shipping emissions on air pollution in the greater North Sea region-Part 2: Scenarios for 2030, Atmos. Chem. Phys., 16(2), 759–776, doi:10.5194/acp-16-759-2016, 2016.

Ng, S. K. W., Loh, C., Lin, C., Booth, V., Chan, J. W. M., Yip, A. C. K., Li, Y. and Lau, A. K. H.: Policy change driven by an AIS-assisted marine emission inventory in Hong Kong and the Pearl River Delta, Atmos. Environ., 76, 102–112, doi:10.1016/j.atmosenv.2012.07.070, 2013.

Paxian, A., Eyring, V., Beer, W., Sausen, R. and Wright, C.: Present-day and future global bottom-up ship emission inventories including polar routes, Environ. Sci. Technol., 44(4), 1333–1339, doi:10.1021/es9022859, 2010.

Smith, T.W.P, Jalkanen, J.-P., Anderson, B.A., Corbett, J.J., Faber, J., Hanayama, S., O'Keeffe, E., Parker, S., Johansson, L., Aldous, L., Raucci, C., Traut, M., Ettinger, S., Nelissen, D., Lee, D.S., Ng, S., Agrawal, A., Winebrake, J.J., Hoen, M., Chesworth, S. and Pandey, A. (2015). Third IMO GHG Study 2014. International Maritime Organization (IMO). London, UK. Available from: http://www.imo.org/en/OurWork/Environment/PollutionPrevention/AirPollution/, 2014.

Song, S., Ship emissions inventory, social cost and eco-efficiency in Shaghai Yangshan port, Atm. Env., 82, 288-297, http://dx.doi.org/10.1016/j.atmosenv.2013.10.006, 2014.

US Energy Information Administration, https://www.eia.gov/dnav/pet/hist_xls/MCRFPUS1a.xls, accessed March 10th 2017.

Research highlights

- A model (STEAM3) for the assessment of global shipping emissions is presented.
- The modelling is based on ship activities given by AIS, for more than 300,000 ships.
- A route generation algorithm is used to handle large gaps in the AIS-data.
- Data-assimilation is used to assign physically realistic properties for each ship.
- Results for global shipping emissions have been analyzed and presented for 2015.